

Origin and Transformation of Ambient VOCs during a Dust-to-Haze Episode in Northwest China

Yonggang Xue^{1,2,3,4}, Yu Huang^{1,2,3,4*}, Steven Sai Hang Ho^{1,2,5}, Long Chen^{1,2,3,4}, Liqin Wang^{1,2,3,4}, Shuncheng Lee⁶, Junji Cao^{1,2,3,4*},

¹Key Lab of Aerosol Chemistry & Physics, Institute of Earth Environment, Chinese Academy of Sciences, Xi'an 7 0061, China

²State Key Lab of Loess and Quaternary Geology (SKLLQG), Institute of Earth Environment, Chinese Academy of Sciences, Xi'an 710061, China

³Shaanxi Key Laboratory of Atmospheric and Haze-fog Pollution Prevention, Institute of Earth Environment, Chinese Academy of Sciences, Xi'an 710061, China

⁴CAS Center for Excellence in Quaternary Science and Global Change, Xi'an, 710061, China.

⁵Division of Atmospheric Sciences, Desert Research Institute, Reno, Nevada, USA

⁶Department of Civil and Environmental Engineering, The Hong Kong Polytechnic University, Hung Hom, Hong Kong, China

Correspondence to: Yu Huang (huangyu@ieecas.cn)

Junji Cao (cao@loess.llqg.ac.cn)

Abstract. High contribution of secondary organic aerosol to the loading of fine particle pollution in China highlights the roles of volatile organic compounds oxidation. Therein, particulate active metallic oxides in dust, like TiO₂ and Fe ions, were proposed to influence the photochemical reactions of ambient VOCs. A case study was conducted at an urban site in Xi'an, northwestern China, to investigate the origin and transformation of VOCs during a windblown dust-to-haze pollution episode, and the assumption that dust would enhance the oxidation of VOCs was verified. Local vehicle exhaust (24.76%) and biomass burning (18.37%) were found to be the two largest contributors to ambient VOCs. In the dust pollution period, sharp decrease of VOCs loading and aging of their components were observed. Simultaneously, the secondary oxygenated VOCs fraction (i.e., methylglyoxal) increased. Source strength, physical dispersion, and regional transport were eliminated from the major factor for the variation of ambient VOCs. In another aspect, about 2 and 3 times increase of the loading of Iron (Fe) and titanium (Ti) was found in the airborne particle, together with fast decrease of trans-/cis-2-butene ratios which demonstrated that dust can accelerate the oxidation of ambient VOCs and formation of SOA precursors.

33 **1 Introduction**

34 Secondary aerosols are important components of fine particles in China, which could contribute to about
35 30 to 77 percent of PM_{2.5} loading, therein, secondary organic aerosols (SOA) take about half of the
36 loading (Huang et al., 2014). Guo et al. (2014) believed that gaseous emissions of volatile organic
37 compounds (VOCs) and nitrogen oxides (NO_x) were responsible for the large secondary PM formation.
38 Laboratory experiments found OH-initiated oxidation of m-xylene could cause the coating thickness of
39 black carbon, which further induced increase of particle size (1.5 to 10.4 times) and effective density
40 (from 0.43 to 1.45 g cm⁻³) (Guo et al., 2016).

41 Solid-gas heterogeneous reactions would cause the transformation of gaseous pollutants and change
42 the property of particles (Zhang et al., 2000; Zhang et al., 2003; He et al., 2014). Recently, the oxidation
43 of organic and inorganic gas on particles surface through the transitional-metal-catalyzed chain reaction
44 was frequently found to play important roles on the transformation of ambient gas pollutants (Chu et al.,
45 2019). Mineral dust is the most important sources of the transitional-metal, like Iron (Fe) and titanium
46 (Ti), in the natural environment (Chen et al., 2012). In addition, mineral dust is one kind of the most
47 abundant components of the global airborne PM, and about 1600 to 2000 Tg of mineral dust is
48 transformed to aerosols annually from major deserts (Ginoux et al., 2001). Furthermore, the surface of
49 mineral dust provides plenty of reactive sites for multiple atmospheric trace gas reactions (Cwiertny et
50 al., 2008). As a result, dust was viewed to serve as catalyst for reactive gas, and modify the photochemical
51 processes (Dentener et al., 1996; Dickerson et al., 1997).

52 With the controlled experiment of sulfate formation on mineral dust, Zhang et al. (2019) found that
53 under appropriate humidity and particle acidity, surface transitional-metal-catalyzed chain reaction
54 together with nitrate would highly accelerate the sulfate's formation on the surface of mineral dust
55 (Zhang et al., 2019). In another aspect, gas-solid heterogeneous photochemical reactions of organic
56 compounds were also reported on the illuminated surface of semiconductor metal oxides in the natural
57 environment, in particular TiO₂ (Chen et al., 2012). Co-existence heterogeneous photochemical reactions
58 of SO₂, NO₂ and VOCs on the surface of mineral dust were investigated in recent years. Both synergistic
59 and suppress effects of VOCs on the formation of sulfate were found, which indicated the competition
60 of reactive oxygen species and active sites between VOCs and inorganic gas pollutants (Chu et al., 2019;

61 Song et al., 2019). In addition, oxidized products, like formate and acetate species, were observed in the
62 co-existence reaction, which highlight the possibility of further oxidation of VOCs on the mineral dust
63 (He et al., 2014). In northwestern China, dust from both local sources and long-range transport is one of
64 the most important components of particulate matter of $< 2.5 \mu\text{m}$ in diameter ($\text{PM}_{2.5}$) (Huang et al., 2014).
65 Xi'an has a population of ~ 8 million (Feng et al., 2016). The sharp increase of vehicles and other human
66 activities has led to high emissions of VOCs and NO_x (Li et al., 2017). Observations showing
67 simultaneous high dust loading and elevated VOCs and NO_x concentrations suggest possible impacts
68 from heterogeneous reaction on dust particles (Huang et al., 2014; Li et al., 2017). The present study was
69 conducted to investigate the origin and transformation of ambient VOCs with severe dust-to-haze episode
70 in winter. The transformation and the related chemical processing of ambient VOCs and the related
71 changes in the composition of $\text{PM}_{2.5}$ were studied, within typical windblown dust-to-haze episodes. The
72 potential pathway of VOCs oxidation in the windblown dust-to-haze formation process was explored.

73 **2 Materials and Methods**

74 **2.1 Sampling site**

75 An observation site (E $109^\circ 00' 7''$, N $34^\circ 13' 22''$) managed by Xi'an Jiaotong University was used in
76 this study (Figure 1). All sampling equipment was deployed on the rooftop of a 15-m tall academic
77 building. No obvious stationary pollution sources were found nearby, and the location can be considered
78 as a typical urban location in Xi'an (Zhang et al., 2015a).

79 **2.2 Field Sampling**

80 Severe dust-to-haze episode was observed in Xi'an and the surrounding areas from 8 November to 12
81 November in 2016, and samples was continuously collected during this period to investigate the chemical
82 compositions of both VOCs and fine PM. A total of 57 non-methane VOCs species (i.e., $\text{C}_2\text{-C}_{12}$ saturated
83 and unsaturated aliphatic and aromatic VOCs) were sampled hourly into offline multi-bed adsorbent
84 tubes; the measured 57 VOCs were defined as VOC_{PAMS} . The loaded tubes were analyzed using a thermal
85 desorption and gas chromatography/mass spectrometry (TD-GC/MS) method. In previous
86 developmental work, humidity and temperature during sampling were found to impact significantly on
87 the analyses; for this study, all sample collections were made under optimized conditions (Ho et al., 2017;

88 Ho et al., 2018). Sixteen airborne carbonyls (including mono- and dicarbonyls) were collected over
89 diurnal cycles (i.e., 20:00–08:00 local time [LT] and 08:00-20:00 LT) by 2,4-dinitrophenylhydrazine
90 (DNPH) coated-cartridges. Detailed sampling and analytical procedures for VOCs and carbonyls can be
91 found in previous publication (Ho et al., 2017; Dai et al., 2012).

92 PM_{2.5} filter samples were sampled with mini-volume samplers (Model Mini-Vol, Air Metrics Co.,
93 Oregon, USA) by a flow rate of 5 L min⁻¹ (Cao et al., 2005). Fine PM was sampled by 47-mm quartz
94 microfiber filters (Whatman QM/A, Maidstone, UK), and the filters were pre-heated at 900°C for 3-h
95 before sampling. The loaded filters were transferred into clean polystyrene petri dishes and stored in a
96 freezer.

97 **2.3 Chemical Analyses**

98 Analytical procedures for VOC analysis have been described previously (Ho et al., 2017). In brief, the
99 analytes in the adsorbent tubes were firstly desorbed in a thermal desorption unit (Series 2 UNITY-xr
100 system with ULTRA-xr, Markes International, Ltd., UK) coupled to a GC/MS (7890A/5977B, Agilent
101 Technologies, Santa Clara, CA, USA). The loaded tube was transferred into the TD unit and blown with
102 ultra-high purity He gas. The targeted VOCs were desorbed at 330°C within 8 mins, and then refocused
103 onto a cryogenic-trap (U-T1703P-2S, Markes) at -15°C. The targeted VOCs were transferred to a cold
104 GC capillary column head (Rtx®-1, 105 m × 0.25 mm × 1 mm film thickness, Restek Corporation, USA)
105 at -45°C. The chromatographic condition could be found in our previous work (Ho et al., 2017).

106 For carbonyl compounds, the DNPH cartridges were firstly eluted with acetonitrile (HPLC/GCMS
107 grade, J & K Scientific Ltd., Ontario, Canada) (Dai et al., 2012). The extracts were analyzed with a
108 typical high-pressure liquid chromatography (HPLC) system (Series 1200; Agilent Technologies)
109 equipped with photodiode array detector. The column was matched with a 4.6 × 250 mm Spheri-5 ODS
110 5 µm C-18 reversed-phase column (Perkin-Elmer Corp., Norwalk, CT) (Dai et al., 2012; Ho et al., 2011).

111 The particulate organic carbon (OC) and elementary carbon (EC) were analyzed with a DRI model
112 2001 carbon analyzer (Atmoslytic, Inc., Calabasas, CA, USA) (Chow et al., 2007; Chow et al., 1993).
113 Anions (Cl⁻, NO₃⁻, and SO₄²⁻) and cations (Na⁺, NH₄⁺, K⁺, Mg²⁺, and Ca²⁺) in particles were determined
114 in aqueous extracts of the sample filters. Detailed extraction and analytical procedures were presented in

115 a previous publication (Zhang et al., 2011). The abundances of 25 particulate elements (Na, Mg, Al, Si,
116 S, Cl, K, Ca, Sc, Ti, V, Cr, Mn, Fe, Co, Ni, Cu, As, Se, Br, Sr, Ba, Pb, Ga, Zn) were measured by energy
117 dispersive x-ray fluorescence (ED-XRF) spectrometry (Epsilon 4 ED-XRF, PAN alytical B.V., the
118 Netherlands). The X-ray source was matched with a metal-ceramic X-ray tube with a Rh and Ag anode,
119 and X-ray source was operated at a maximum current of 3mA, and the maximum accelerating voltage of
120 50kV (maximum power 15W).

121 **2.4 Quality Control**

122 The Minimum detection limits (MDLs) of the VOCs were in the range of 0.003–0.042 ppbv with a 3
123 L sampling volume (Table S1). The measurement precision at 2 ppbv was $\leq 5\%$ (Ho et al., 2017; Ho et
124 al., 2018). Three field blank samples were collected within each sampling day, and they were analyzed
125 using the same procedures as those for the ambient air samples. Most target compounds were not detected
126 in the field blanks, and propylene, benzene, and toluene were below their MDLs (< 0.23 g per tube and
127 $< 10\%$ of the arithmetic mean of ambient samples). No breakthrough ($\sim 0\%$) was observed for VOC_{SPAMS}
128 except for C₂–C₃ hydrocarbons, which were $< 10\%$ when the air temperature was $> 30^\circ\text{C}$. The MDLs for
129 the carbonyl target compounds were between 0.009 to 0.067 ppbv at a sampling volume of 3.6 m³.
130 Negligible breakthrough ($< 5\%$) was found under the sampling conditions and flow rates in the field.

131 **3. Results and Discussion**

132 **3.1 Origins of ambient VOCs during Dust and Fine-particle Pollution Events**

133 In the present study, mixing ratios of the sum of non-methane hydrocarbon was 36.0 ± 15.7 ppbv, which
134 was lower comparing to that in Beijing and Guangzhou with values of 51.0 and 47.8 ppbv, respectively.
135 Similar levels of alkenes were seen at the cities of Beijing (9.4 ppbv) and Guangzhou (8.2 ppbv)
136 comparing to that in the present study (9.2 ppbv, Table S2, Ho et al., 2004; Liu et al., 2008b).
137 Unexpectedly, the aromatics were slightly higher in Xi'an (10.3 ppbv) than that in Beijing (9.6 ppbv),
138 and 50% higher than that in Guangzhou (6.8 ppbv, Shao et al., 2009; Zou et al., 2015). Therein, ethylene,
139 ethane, toluene, iso-pentane, propane, n-butane, iso-butane, propylene, n-pentane, and benzene were the
140 most 10 abundant VOC_{SPAMS}. The high fractions of these markers reflect strong emissions from traffic
141 and coal combustion or from biomass burning (Liu et al., 2008a; Ho et al., 2009; Huang et al., 2015; Fan

142 et al., 2014; Zhang et al., 2015c). Previous studies found higher contributions of non-fossil sources to
143 carbonaceous aerosols in Xi'an, as compared with Beijing (Ni et al., 2018). Generally, non-fossil
144 emissions mainly originate from biomass burning (Ni et al., 2018), and the higher contribution of non-
145 fossil sources to carbonaceous in Xi'an would indicate remarkable biomass burning activities exist in
146 Xi'an and the surrounding areas (Huang et al., 2014; Xu et al., 2016).

147 Receptor models and correlations between individual VOCs have been used for source assessments.
148 In this study, significant correlation ($R^2=0.62$, $p<0.05$, slope of 1.59) was found for a least-squares
149 regression between toluene and benzene (Figure S1). The ratio of toluene to benzene (T/B) ratio has been
150 shown to different among combustion sources; for example, Liu et al. (2006) reported T/B ratios of 1.5-
151 2.0 in gasoline-related emissions collected in a tunnel. In contrast, T/B ratios ranged from 0.23-0.68 and
152 0.13-0.71 for biomass burning and coal combustion, respectively (Zhang et al., 2015c). The T/B ratios
153 in our samples ($R^2=0.62$, $p<0.05$, slope of 1.59) implied a strong impact from traffic on the ambient
154 VOCs in Xi'an. Significant correlations ($p<0.05$) were observed among C_3 - C_5 alkanes, with propane
155 versus n-butane ($R^2=0.75$, slope=0.91), n-pentane versus iso-pentane ($R^2=0.85$, slope=0.35), and trans-
156 2-butene versus cis-2-butene ($R^2=0.99$, slope=0.84)(Figure S1). The observed ratio of propane to n-
157 butane in Xi'an was 1.1, which is close to that (1.36) observed in the tunnel study cited above (Liu et al.,
158 2008). High loadings of n-pentane and iso-pentane are indicative of unburned vehicular emissions, and
159 Liu et al., (2008) reported a ratio of iso-pentane/n-pentane of 3 in tunnel air, which is consistent with the
160 slope of 2.85 found in the present study. The ratios of T/B, trans-/cis-2-butene, propane/n-butane and n-
161 pentane/iso-pentane indicated that gasoline emission was dominated sources of ambient VOCs, and the
162 source apportionment by PMF model result, and the detail description of source apportionment will be
163 carried out in the following section.

164 PMF model was used to identify the major pollution sources: the data input to the model were the
165 mixing ratios and uncertainties in the VOCs mixing ratios for all valid samples collected during the study.
166 Five sources were identified (Figure S2), and the detail process of source apportionment were given in
167 the supporting information. Biomass burning and gasoline exhaust were the two most significant
168 pollution sources, contributing 24.76% and 18.37%, respectively. The combustion of LPG and CNG
169 (24.67%), diesel exhaust (15.28%), coal combustion (16.92%) also were found to be important sources
170 of ambient VOCs (Figure S2). Biomass is commonly used for heating and cooking in rural areas of the
171 basin in winter due to its low cost compared with natural gas and electricity. Consistent with our results,

172 previous studies found high contribution of biomass burning and gasoline exhaust to the organic aerosol
173 in Guanzhong Basin(Cao et al., 2005).

174 Clear air conditions occurred at the beginning of the sampling period, but severe dust and fine-particle
175 pollution events were observed afterward. The high dust event was defined by loading of particulate
176 matter $\leq 10 \mu\text{m}$ in aerodynamic diameter (PM_{10}) between 300 and 500 $\mu\text{g m}^{-3}$, and these conditions
177 occurred from 12:00 LT on 9 November to 13:00 LT on 10 November. The abatement of dust before the
178 fine particle pollution event is referred to as the transition period (i.e., $\text{PM}_{10} < 300 \mu\text{g m}^{-3}$ and $\text{PM}_{2.5} <$
179 $100 \mu\text{g m}^{-3}$). The loading of $\text{PM}_{2.5}$ subsequently increased, and heavy fine particle pollution ($\text{PM}_{2.5} > 100$
180 $\mu\text{g m}^{-3}$) occurred after 18:00 LT on 11 November.

181 Ratios of individual VOCs can be used to identify the origins of the compounds and to study
182 atmospheric aging processes due to the special composition of VOCs in a typical source and the different
183 lifetime of VOCs species (Xue et al., 2017; Zhang et al., 2015c). In addition, influences from
184 meteorological variation and atmospheric transport also need to be considered when the potential sources
185 of the compounds in ambient air are characterized. To investigate the impacts of air mass transport on
186 VOCs concentrations, we calculated air-mass back trajectories using the NOAA HYSPLIT model for the
187 dust event (Figure S4a) and for the fine-particle pollution episode (Figure S4b). The trajectories were
188 calculated at an arrival height of 500 m above ground at the observation site. In view of the short
189 atmospheric lifetimes of VOCs (for example, isoprene, ~ 1.4 h; propylene, ~ 5.3 h; toluene, 2.1 d)
190 (Atkinson and Arey, 2003), 24-h back trajectories were used for this assessment.

191 Clear different air masses back trajectories and VOCs ratios were observed between dust pollution and
192 haze pollution periods. From 9 November to 10 November (in dust pollution period), the air mass
193 reaching Xi'an passed over areas to the west of the city (i.e., Gansu Province and Ningxia Autonomous
194 Region) through long range transport; after 11 November (formation of haze), the transport of air mass
195 was mainly limited to areas around southern Xi'an. Differences in the chemical compositions of ambient
196 VOCs in the dusty versus in the haze event can clearly be seen (Figure 2) in the ratios of toluene to
197 benzene (T/B) and m, p-xylene to ethylbenzene (X/E). During the clear and dusty periods, the T/B and
198 X/E ratios varied significantly with time of day; that is, the highest values for T/B (4.5–9.0) and X/E
199 (0.98–1.05) were seen during rush hour (07:00–09:00 LT and 17:00–19:00 LT), while the lowest values
200 (0.50–1.95 for T/B, and 0.89–0.96 for X/E) occurred in the early afternoon (i.e., 14:00–15:00 LT). The
201 timings of the high T/B and X/E ratios suggest that fresh emissions from local traffic were the major

202 source for the ambient VOCs, and this implies that long-range transport did not have a strong impact on
203 the ambient VOCs during the clear or dusty parts of the study (Ho et al., 2004; Liu et al., 2008a). While
204 during the transitional and fine PM pollution period, both T/B and X/E varied but at relatively lower
205 values compared with the earlier parts of the study (T/B, 3.33 ± 1.97 , 2.21 ± 0.86 , 1.91 ± 0.74 , 2.01 ± 0.56 in
206 clear, dust, transitional and fine particle pollution periods, respectively; X/E, 1.00 ± 0.05 , 1.05 ± 0.12 ,
207 0.93 ± 0.17 , 0.95 ± 0.13 in clear, dust, transitional and fine particle pollution periods, respectively). These
208 synchronous lower values of T/B and X/B in transitional and fine particle pollution periods were
209 indicative of aged air masses (Zhang et al., 2015c; Xue et al., 2017; Warneke et al., 2013).

210 Variations in the air mass transport pathway, and T/B or X/E during different sampling periods (clear,
211 dust, transitional, fine particle pollution) confirmed that ambient VOCs were fresh in the clear and dust
212 periods, but relatively aged during the transitional and fine particle pollution periods (Zhang et al., 2015c;
213 Xue et al., 2017; Warneke et al., 2013). This indicates that the long-range transport of air mass had a
214 relatively weak influence on the ambient VOCs even during the high dust period. Otherwise, composition
215 of ambient VOCs should be relative aged due to long exposure time with dust transport. Indeed,
216 emissions from local vehicular exhausts and biomass burning in Xi'an and the surrounding areas were
217 the main contributors to ambient VOCs throughout our study.

218 **3.2 Transformation of VOCs between Dust and Fine Particle Events**

219 With the shading of dust, level of ambient VOCs decreased with time, and the low concentrations
220 (average of 19.0 ppbv, 8.3 to 33.9 ppbv) were observed from 13:00 LT on 10 November and 01:00 LT
221 on 11 November (Figure 3). During the fine particle pollution period (12–13 November), the Σ
222 $\text{VOC}_{\text{SPAMS}}$ increased, reaching an average of 38.0 ppbv in the last 24 h, compared with 19.0 ppbv in the
223 transitional period and 21.5 ppbv in the first 12 h of the fine particle pollution episode (Figure 3). This
224 buildup of VOCs can be explained by weak dispersion and relatively shallow boundary layers (400–1000
225 m) during the event (Figure 3). In addition, during this transition period, much lower ratios of T/B and
226 X/E were observed in comparison with those in other periods (as mentioned in the part 3.1.2). We
227 propose the possibility that windblown dust which include sustainable TiO_2 can influence the
228 atmospheric photochemistry of VOCs, which would accelerate the oxidation of ambient VOCs (Chu et
229 al. 2019; Nie et al., 2014).

230 While changes in the emission sources and their strengths, physical dispersion, regional transport, and
231 aging of air masses all could affect VOC levels and composition (Xue et al., 2013; Xue et al., 2017). As
232 a result, to evaluate aging of ambient VOCs in different period, the impact of dust on the transform of
233 ambient VOCs, and the relative processes, the mentioned factors should be fully considered.

234 To evaluate the impact of sources types on the variation of VOCs in the dust-to-haze episode, diurnal
235 variation of VOCs was depicted. During the clear and dusty periods—and similar to the trends in T/B
236 and X/E ratios—peaks in $\Sigma \text{VOC}_{\text{SPAMS}}$ were seen from 17:00 to 20:00 LT and from 09:00 to 12:00 LT
237 (Figure 3), which highlighted the impacts of local traffic emission (Liu et al., 2008a; Huang et al., 2015).
238 And 1,3-Butadiene is often used as marker of gasoline-powered motor vehicles (Huang et al., 2015),
239 while ethane is key chemical marker for biomass and coal combustion (Liu et al., 2008a). Time series
240 plots of 1,3-butadiene and ethane (Figure S5) show that peaks in 1,3-butadiene mostly occurred during
241 rush hour, while higher concentrations of ethane were seen during the night. These results support the
242 conclusions that there were strong impacts from gasoline-powered motor vehicles in the daytime and
243 from biomass burning or coal combustion for heating at night. In addition, winter heating activities was
244 relatively active because of low temperatures during the transitional period, and this limited the
245 possibility of reduced emission amounts. Hence the variations of sources strength was eliminated from
246 the major factor caused the extremely low concentration and relative aged composition of ambient VOCs.

247 Variation of physical dispersion was also eliminated. With the shading of dust transport, shallow
248 boundary layers were observed in the transitional period. For the clear and dust transport period, the
249 boundary layer between 08:00 to 14:00 was relatively deep (1150–1500 m). In contrast, the boundary
250 layer height decreased sharply to < 800 m on 11 November in transitional period. This limited the
251 possibility that diffusion caused the sharp decrease of ambient VOCs in the transitional period.

252 Significant impact of air mass input was eliminated. Input of air mass would certainly cause the
253 variations of VOCs' composition and loading (Xue et al., 2014). In the present study, long range transport
254 of air masses had limited impacts on the characteristic of ambient VOCs during the sampling period. In
255 another aspect, relative active VOCs would be firstly degraded, hence composition of ambient VOCs
256 would be aging with long range transport (Ho et al., 2009; Xue et al., 2017). While in the present study,
257 as mentioned above, composition of ambient VOCs was relative fresh under long range transport of air
258 mass (within dust transport). In contrast, VOCs composition was relatively aged under the air mass that
259 limited with Xi'an and the surrounding area (transitional period). This phenomenon indicated that

260 regional transport cannot be the major factor inducing the relative aged composition and excess low
261 loading of the ambient VOCs in the transitional period.

262 Synchronous changes of the VOCs isomeride were found in the windblown dust-to-haze episode,
263 which supplied the evidence of the accelerated photochemistry reactions. In the present study, we
264 found fast decrease of trans-/cis-2-butene ratio within dust transporting, which confirmed the accelerated
265 photochemical reactions of ambient VOCs (Figure 4). Trans-2-butene and cis-2-butene are two
266 isomerides that mostly emitted from same sources (Zheng et al., 2017; Zhang et al., 2015b). While trans-
267 2-butene has higher photochemical reactions rate with OH radical in the atmosphere ($k_{OH} 6.40 \times 10^{-11} s^{-1}$)
268 than cis-2-butene ($k_{OH} 5.64 \times 10^{-11} s^{-1}$) (Perring et al., 2013), hence trans-/cis-2-butene ratio would
269 decrease with the photochemical reactions (Zhang et al., 2015b). Firstly, relative higher trans-/cis-2-
270 butene ratios were observed in the rush hours (evening rush hours 17:00-20:00, morning rush hours
271 07:00-10:00) (Figure 4), which indicated fresh emission from local traffic activities (Zhang et al., 2015b).
272 In addition, sharp decrease of trans-/cis-2-butene ratio was observed from late half of windblown dust
273 period to the end of transitional period (Figure 4). The quickly shrinking of trans-2-butene comparing to
274 cis-2-butene in the dust pollution period indicated that oxidation of ambient VOCs was accelerated in
275 the period with high loading of the suspending dust particles (Zhang et al., 2015b).

276 Significant increase of particulate active metals was found in dust pollution period, which further
277 verified the promotion of dust on the heterogeneous reactions. Previous study found that mineral dust
278 can affect the chemistry of the atmosphere by scavenging gaseous compounds (Zhang et al., 2000; Chen
279 et al., 2012); it can also promote heterogeneous reactions of atmospheric substances, including VOCs,
280 because the particle surfaces can provide sites for photo-catalytic reactions (Cwiertny et al., 2008; Ndour
281 et al., 2009). In the present study, ferrum (Fe) and titanium (Ti) contents of the particulate increased
282 significantly within the period with dust transport (Figure 5). In detail, content of Fe increased from 19.3
283 $\mu g m^{-3}$ in clear days to 40.8 $\mu g m^{-3}$ in dust pollution days, and the content of Ti increased from 0.92 to
284 2.98 $\mu g m^{-3}$. Hence, huge increase of the Ti and Fe concentrations in particulate phase during the period
285 of dust pollution days could possibly promote the gas-solid photochemical reaction of the ambient VOCs,
286 which would reasonably ascribe the relative low level and aged composition of ambient VOCs in this
287 period (Chu et al., 2019; He et al., 2014; Song et al., 2019).

288 **3.3 Variation of carbonyl compounds between dust to fine particle pollution periods: further**
289 **formation oxygenated VOCs with aging of primary VOCs**

290 Aging of primary VOCs and formation of carbonyl compounds were observed synchronously, as the
291 fine-particle pollution event developed (Figure 3; Figure 6a). As discussed above, relatively low T/B and
292 X/E values were observed during the transitional and fine PM periods after the dust event (Part 3.2). In
293 our study, the carbonyl levels increased after the clear and dusty periods, and the highest levels were
294 seen during the fine particle pollution event (Figure 6a). Carbonyl compounds are produced from both
295 the primary sources and form through secondary processes (Dai et al., 2012; Duan et al., 2012), and we
296 found higher carbonyl concentrations during daytime than at night (Figure 6a). This is consistent with
297 previous studies in Xi'an (Dai et al., 2012), which confirmed the secondary formation of carbonyl
298 compound under sunlight illumination.

299 Methylglyoxal is generally considered to be a secondary species, while acetone is mainly from primary
300 emissions; the ratio of acetone to methylglyoxal (A/M) has been used as an indicator of air mass aging
301 (Dai et al., 2012; Liu et al., 2006). In the present study, A/M ranged from 12 to 14 during the clear and
302 first half of dusty periods but then dropped sharply and stayed between 6 and 9 during the later parts of
303 dust pollution period, transitional and the high PM event (Figure 6a). Increases in the abundances of
304 carbonyl compounds and lower A/M ratios suggested relatively stronger aging of the air masses, this is
305 further evidence of fast degradation of VOCs in the late half of the windblown dust event, and the primary
306 VOCs were oxidized and served as precursors of SOA. In consequence, composition of particles changed
307 with oxidation of ambient VOCs across the sampling periods.

308 **3.4 Variations of PM_{2.5} Chemical Composition during Dusty and Fine PM Pollution Periods**

309 Significant variations of water-soluble inorganic ions, OC, and EC were observed diurnally and
310 between dust and fine particle pollution events (Figure 6b, c). For instance, the concentrations of NO₃⁻
311 were relatively high in the daytime, while K⁺ and Cl⁻ were more abundant at night. The diurnal cycles
312 can be explained by the formation of secondary particles through photochemical processes during the
313 daytime and by the impacts from biomass and coal burning for heating at night (Dai et al., 2012; Zhang
314 et al., 2018; Cong et al., 2015). The concentrations of Ca²⁺, Mg²⁺, and Na⁺, which are typically associated
315 with dust in inland areas (Wu et al., 2011), increased sharply during the dusty period, and then declined
316 rapidly afterwards.

317 As discussed, the apparent contribution of VOCs to the formation of SOAs increased when the dusty
318 conditions transitioned into a fine-particle pollution event. Temporal changes in the chemical
319 composition of PM_{2.5} are consistent with this suggestion. During the fine-particle pollution period, both
320 the concentrations of secondary ions, particularly NO₃⁻, increased as the haze event developed. A similar
321 trend was seen for OC (Figure 6b), and content of particulate OC increased from 11.1 since dust event
322 period to 47.1 in the haze period. In another aspect, the ratio of OC/EC increased from 1.3 to 4.9 in the
323 dust-to-haze episode. The previous studies on the characterization of particles from traffic emission
324 reported OC/EC values in the range of 0.28 to 0.92 in the diesel vehicles, and the OC/EC values were
325 reported >2 in the gasoline vehicles (Cadle et al., 1999; Huang et al., 2006) (). In addition, the OC/EC
326 was reported in the range of 0.9 to 1.6 in the urban region in the city of Guangzhou (Tao et al., 2019). In
327 the present study, the consistent increase of OC/EC would prove the formation of SOA in the dust-to-
328 haze episode. Combined with the findings regarding the compositions of VOCs and PM_{2.5}, these results
329 indicate that the reactions of VOCs led to the formation of SOA, and in so doing contributed to the fine
330 particle pollution.

331 **4. Conclusion**

332 Comprehensive field work was carried out to investigate the origin and transform of VOCs within the
333 dust-fine particles pollution periods in winter with the city of Xi'an. And the assumption of promotions
334 of dust on the heterogeneous reactions of VOCs was further verified. Local vehicle exhaust (40%) and
335 heating activities (41%) were found to be the most important sources of the ambient VOCs in Xi'an
336 within winter, while long range transport air mass has limited impacts. Within the period of dust transport,
337 loading of ambient VOCs decreased sharply from the late half period (average of 38 ppbv in dust period
338 to average of 19 ppbv in transitional period), and the lowest concentration was observed in the transitional
339 period (8 ppbv), in accordance with aging of primary VOCs. In addition, loading and proportion of
340 secondary VOCs in gaseous phase and secondary ions and organic carbon in particulate phase increased
341 with the aging of primary VOCs. Source strength, physical dispersion, and regional transport were
342 eliminated from the major factor for the variation of the ambient VOCs. On another aspect, sharp increase
343 of active metals concentrations (Ti and Fe) and fast decrease of trans-/cis-2-butene ratio was observed
344 from the late half of dust transport period (1.21 to 0.65). In consequence, we conclude that windblown

345 dust might accelerate the gas-solid heterogeneous reactions of atmospheric VOCs, and further induced
346 the formation of SOA precursors.

347

348 *Data availability.* All of the research data have been included in the supplement.

349

350 *Supplement.* The following information is provided in the Supplement: Sampling procedures, Chemical
351 Analysis, Source characterization, Figure S1-S5, Table S1-S2.

352

353 *Author contributions.* YX designed the study. YX and YH wrote the paper. SH, JC and SL revised the
354 manuscript, LC and LW analyzed the data. All authors reviewed and commented on the paper.

355

356 *Competing interests.* The authors declare that they have no conflict of interest.

357

358 *Acknowledgements.* This research was financially supported by the National Key Research and
359 Development Program of China (Grant No. 2016YFA0203000), and the National Science Foundation of
360 China (Grant No. 41701565, 21661132005, 41573138). Yu Huang was also supported by the “Hundred
361 Talent Program” of the Chinese Academy of Sciences. The data used are listed in the supplements.

362 **References**

363 Atkinson, R., and Arey, J.: Atmospheric Degradation of Volatile Organic Compounds, Chem. Rev., 103,
364 4605-4638, <https://doi.10.1021/cr0206420>, 2003.

365 Cadle SH, Mulawa PA, Hunsanger EC, Nelson K, Ragazzi RA, Barrett R, et al. Composition of light-
366 duty motor vehicle exhaust particulate matter in the Denver, Colorado area. Environ. Sci. Technol., 33:
367 2328-2339, <https://doi.org/10.1021/es9810843>, 1999.

368 Cao, J., Wu, F., Chow, J., Lee, S., Li, Y., Chen, S., An, Z., Fung, K., Watson, J., and Zhu, C.:
369 Characterization and source apportionment of atmospheric organic and elemental carbon during fall and
370 winter of 2003 in Xi'an, China, Atmos. Chem. Phys., 5, 3127-3137, [https://doi.org/10.5194/acp-5-3127-](https://doi.org/10.5194/acp-5-3127-2005)
371 2005, 2005.

372 Chen, H., Nanayakkara, C. E., and Grassian, V. H.: Titanium Dioxide Photocatalysis in Atmospheric
373 Chemistry, *Chem. Rev.*, 112, 5919-5948, <https://doi.10.1021/cr3002092>, 2012.

374 Chow, J. C., Watson, J. G., Pritchett, L. C., Pierson, W. R., Frazier, C. A., and Purcell, R. G.: The dri
375 thermal/optical reflectance carbon analysis system: description, evaluation and applications in U.S. Air
376 quality studies, *Atmos. Environ., Part A. General Topics*, 27, 1185-1201, [https://doi.org/10.1016/0960-](https://doi.org/10.1016/0960-1686(93)90245-T)
377 1686(93)90245-T, 1993.

378 Chow, J. C., Watson, J. G., Chen, L. W. A., Chang, M. C. O., Robinson, N. F., Trimble, D., and Kohl,
379 S.: The IMPROVE_A Temperature Protocol for Thermal/Optical Carbon Analysis: Maintaining
380 Consistency with a Long-Term Database, *J. Air Waste Manage.*, 57, 1014-1023,
381 <https://doi.org/10.3155/1047-3289.57.9.1014>, 2007.

382 Chu, B., Wang, Y., Yang, W., Ma, J., Ma, Q., Zhang, P., Liu, Y., and He, H.: Effects of NO₂ and C₃H₆
383 on the heterogeneous oxidation of SO₂ on TiO₂ in the presence or absence of UV irradiation, *Atmos.*
384 *Chem. Phys. Discuss.*, 2019, 1-20, <https://doi.org/10.5194/acp-2019-532>, 2019.

385 Cong, Z., Kang, S., Kawamura, K., Liu, B., Wan, X., Wang, Z., Gao, S., and Fu, P.: Carbonaceous
386 aerosols on the south edge of the Tibetan Plateau: concentrations, seasonality and sources, *Atmos. Chem.*
387 *Phys.*, 15, 1573-1584, <https://doi.org/10.5194/acp-15-1573-2015>, 2015.

388 Cwiertny, D. M., Young, M. A., and Grassian, V. H.: Chemistry and photochemistry of mineral dust
389 aerosol, *Annu. Rev. Phys. Chem.*, 59, 27-51, [https://doi.](https://doi.org/10.1146/annurev.physchem.59.032607.093630)
390 [org/10.1146/annurev.physchem.59.032607.093630](https://doi.org/10.1146/annurev.physchem.59.032607.093630), 2008.

391 Dai, W. T., Ho, S. S. H., Ho, K. F., Liu, W. D., Cao, J. J., and Lee, S. C.: Seasonal and diurnal variations
392 of mono- and di-carbonyls in Xi'an, China, *Atmos. Res.*, 113, 102-112,
393 <http://dx.doi.org/10.1016/j.atmosres.2012.05.001>, 2012.

394 Dentener, F. J., Carmichael, G. R., Zhang, Y., Lelieveld, J., and Crutzen, P. J.: Role of mineral aerosol
395 as a reactive surface in the global troposphere, *J. Geophys. Res.-Atmos.*, 101, 22869-22889,
396 <https://doi:10.1029/96JD01818>, 1996.

397 Dickerson, R. R., Kondragunta, S., Stenchikov, G., Civerolo, K. L., Doddridge, B. G., and Holben, B.
398 N.: The Impact of Aerosols on Solar Ultraviolet Radiation and Photochemical Smog, *Science*, 278, 827,
399 <https://doi:10.1126/science.278.5339.827>, 1997.

400 Duan, J., Guo, S., Tan, J., Wang, S., and Chai, F.: Characteristics of atmospheric carbonyls during haze
401 days in Beijing, China, *Atmos. Res.*, 114, 17-27, <http://dx.doi.org/10.1016/j.atmosres.2012.05.010>, 2012.

402 Fan, R., Li, J., Chen, L., Xu, Z., He, D., Zhou, Y., Zhu, Y., Wei, F., and Li, J.: Biomass fuels and coke
403 plants are important sources of human exposure to polycyclic aromatic hydrocarbons, benzene and
404 toluene, *Environ. Res.*, 135, 1-8, <http://dx.doi.org/10.1016/j.envres.2014.08.021>, 2014.

405 Feng, T., Bei, N. F., Huang, R. J., Cao, J. J., Zhang, Q., Zhou, W. J., Tie, X. X., Liu, S. X., Zhang, T.,
406 Su, X. L., Lei, W. F., Molina, L. T., and Li, G. H.: Summertime ozone formation in Xi'an and surrounding
407 areas, China, *Atmos. Chem. Phys.*, 16, 4323-4342, <http://doi.org/10.5194/acp-16-4323-2016>, 2016.

408 Ginoux, P., Chin, M., Tegen, I., Prospero, J. M., Holben, B., Dubovik, O., and Lin, S. J.: Sources and
409 distributions of dust aerosols simulated with the GOCART model, *J. Geophys. Res.-Atmos.*, 106, 20255-
410 20273, <http://doi.10.1029/2000jd000053>, 2001.

411 Guo, S., Hu, M., Zamora, M. L., Peng, J. F., Shang, D. J., Zheng, J., Du, Z. F., Wu, Z., Shao, M., Zeng,
412 L. M., Molina, M. J., and Zhang, R. Y.: Elucidating severe urban haze formation in China, *Proc. Natl.*
413 *Acad. Sci. USA*, 111, 17373-17378, <https://doi.org/10.1073/pnas.1419604111>, 2014.

414 Guo, S., Hu, M., Lin, Y., Gomez-Hernandez, M., Zamora, M. L., Peng, J., Collins, D. R., and Zhang, R.:
415 OH-Initiated Oxidation of m-Xylene on Black Carbon Aging, *Environ. Sci. Technol.*, 50, 8605-8612,
416 <http://doi.org/10.1021/acs.est.6b01272>, 2016.

417 He, H., Wang, Y. S., Ma, Q. X., Ma, J. Z., Chu, B. W., Ji, D. S., Tang, G. Q., Liu, C., Zhang, H. X., and
418 Hao, J. M.: Mineral dust and NO_x promote the conversion of SO₂ to sulfate in heavy pollution days, *Sci.*
419 *Rep.-UK.*, 4, <http://doi.10.1038/srep04172>, 2014.

420 Ho, K. F., Lee, S. C., Guo, H., and Tsai, W. Y.: Seasonal and diurnal variations of volatile organic
421 compounds (VOCs) in the atmosphere of Hong Kong, *Sci. Total. Environ.*, 322, 155-166,
422 <http://dx.doi.org/10.1016/j.scitotenv.2003.10.004>, 2004.

423 Ho, K. F., Lee, S. C., Ho, W. K., Blake, D. R., Cheng, Y., Li, Y. S., Ho, S. S. H., Fung, K., Louie, P. K.
424 K., and Park, D.: Vehicular emission of volatile organic compounds (VOCs) from a tunnel study in Hong
425 Kong, *Atmos. Chem. Phys.*, 9, 7491-7504, <http://doi.org/10.5194/acp-9-7491-2009>, 2009.

426 Ho, S. S. H., Ho, K. F., Liu, W. D., Lee, S. C., Dai, W. T., Cao, J. J., and Ip, H. S. S.: Unsuitability of
427 using the DNPH-coated solid sorbent cartridge for determination of airborne unsaturated carbonyls,
428 *Atmos. Environ.*, 45, 261-265, <http://doi.org/10.1016/j.atmosenv.2010.09.042>, 2011.

429 Ho, S. S. H., Chow, J. C., Watson, J. G., Wang, L., Qu, L., Dai, W., Huang, Y., and Cao, J.: Influences
430 of relative humidities and temperatures on the collection of C₂-C₅ aliphatic hydrocarbons with multi-

431 bed (Tenax TA, Carbograph 1TD, Carboxen 1003) sorbent tube method, *Atmos. Environ.*, 151, 45-51,
432 <http://dx.doi.org/10.1016/j.atmosenv.2016.12.007>, 2017.

433 Ho, S. S. H., Wang, L., Chow, J. C., Watson, J. G., Xue, Y., Huang, Y., Qu, L., Li, B., Dai, W., Li, L.,
434 and Cao, J.: Optimization and evaluation of multi-bed adsorbent tube method in collection of volatile
435 organic compounds, *Atmos. Res.*, 202, 187-195, <https://doi.org/10.1016/j.atmosres.2017.11.026>, 2018.

436 Huang, R., Zhang, Y., Bozzetti, C., Ho, K., Cao, J., Han, Y., Daellenbach, K. R., Slowik, J. G., Platt, S.
437 M., Canonaco, F., Zotter, P., Wolf, R., Pieber, S. M., Bruns, E. A., Crippa, M., Ciarelli, G., Piazzalunga,
438 A., Schwikowski, M., Abbaszade, G., Schnelle-Kreis, J., Zimmermann, R., An, Z., Szidat, S.,
439 Baltensperger, U., Haddad, I. E., and Prevot, A. S. H.: High secondary aerosol contribution to particulate
440 pollution during haze events in China, *Nature*, 514, 218-222, <https://doi.org/10.1038/nature13774>, 2014.

441 Huang X, Yu J, He L, Hu M. Size distribution characteristics of elemental carbon emitted from Chinese
442 vehicles: Results of a tunnel study and atmospheric implications. *Environ. Sci. Technol.*, 40: 5355-5360,
443 <https://doi.org/10.1021/es0607281>, 2006.

444 Huang, Y., Ling, Z. H., Lee, S. C., Ho, S. S. H., Cao, J. J., Blake, D. R., Cheng, Y., Lai, S. C., Ho, K. F.,
445 Gao, Y., Cui, L., and Louie, P. K. K.: Characterization of volatile organic compounds at a roadside
446 environment in Hong Kong: An investigation of influences after air pollution control strategies, *Atmos.*
447 *Environ.*, 122, 809-818, <http://dx.doi.org/10.1016/j.atmosenv.2015.09.036>, 2015.

448 Li, B., Ho, S. S. H., Xue, Y., Huang, Y., Wang, L., Cheng, Y., Dai, W., Zhong, H., Cao, J., and Lee, S.:
449 Characterizations of volatile organic compounds (VOCs) from vehicular emissions at roadside
450 environment: The first comprehensive study in Northwestern China, *Atmos. Environ.*, 161, 1-12,
451 <https://doi.org/10.1016/j.atmosenv.2017.04.029>, 2017.

452 Liu, W., Zhang, J., Kwon, J., Weisel, C., Turpin, B., Zhang, L., Korn, L., Morandi, M., Stock, T., and
453 Colome, S.: Concentrations and Source Characteristics of Airborne Carbonyl Compounds Measured
454 Outside Urban Residences, *J. Air Waste Manage.*, 56, 1196-1204,
455 <https://doi.org/10.1080/10473289.2006.10464539>, 2006.

456 Liu, Y., Shao, M., Fu, L., Lu, S., Zeng, L., and Tang, D.: Source profiles of volatile organic compounds
457 (VOCs) measured in China: Part I, *Atmos. Environ.*, 42, 6247-6260,
458 <http://dx.doi.org/10.1016/j.atmosenv.2008.01.070>, 2008a.

459 Liu, Y., Shao, M., Lu, S., Chang, C.-C., Wang, J.-L., and Fu, L.: Source apportionment of ambient
460 volatile organic compounds in the Pearl River Delta, China: Part II, *Atmos. Environ.*, 42, 6261-6274,
461 <https://doi.org/10.1016/j.atmosenv.2008.02.027>, 2008b.

462 Ndour, M., Conchon, P., D'Anna, B., Ka, O., and George, C.: Photochemistry of mineral dust surface as
463 a potential atmospheric renoxification process, *Geophys. Res. Lett.*, 36, 4,
464 <https://doi.org/10.1029/2008gl036662>, 2009.

465 Ni, H., Huang, R., Cao, J., Liu, W., Zhang, T., Wang, M., Meijer, H. A. J., and Dusek, U.: Source
466 apportionment of carbonaceous aerosols in Xi'an, China: insights from a full year of measurements of
467 radiocarbon and the stable isotope C-13, *Atmos. Chem. Phys.*, 18, 16363-16383, [https://doi.10.5194/acp-](https://doi.10.5194/acp-18-16363-2018)
468 18-16363-2018, 2018

469 Nie, W., Ding, A. J., Wang, T., Kerminen, V. M., George, C., Xue, L. K., Wang, W. X., Zhang, Q. Z.,
470 Petaja, T., Qi, X. M., Gao, X. M., Wang, X. F., Yang, X. Q., Fu, C. B., and Kulmala, M.: Polluted dust
471 promotes new particle formation and growth, *Sci. Rep.-UK.*, 4, 6, <https://doi.org/10.1038/srep06634>,
472 2014.

473 Perring, A. E., Pusede, S. E., and Cohen, R. C.: An Observational Perspective on the Atmospheric
474 Impacts of Alkyl and Multifunctional Nitrates on Ozone and Secondary Organic Aerosol, *Chem. Rev.*,
475 113, 5848-5870, <https://doi.org/10.1021/cr300520x>, 2013.

476 Shao, M., Lu, S. H., Liu, Y., Xie, X., Chang, C. C., Huang, S., and Chen, Z. M.: Volatile organic
477 compounds measured in summer in Beijing and their role in ground-level ozone formation, *J. Geophys.*
478 *Res.-Atmos.*, 114, D00G06, <https://doi.org/10.1029/2008jd010863>, 2009.

479 Song, S. J., Gao, M., Xu, W. Q., Sun, Y. L., Worsnop, D. R., Jayne, J. T., Zhang, Y. Z., Zhu, L., Li, M.,
480 Zhou, Z., Cheng, C. L., Lv, Y. B., Wang, Y., Peng, W., Xu, X. B., Lin, N., Wang, Y. X., Wang, S. X.,
481 Munger, J. W., Jacob, D. J., and McElroy, M. B.: Possible heterogeneous chemistry of
482 hydroxymethanesulfonate (HMS) in northern China winter haze, *Atmos. Chem. Phys.*, 19, 1357-1371,
483 <https://doi.10.5194/acp-19-1357-2019>, 2019.

484 Tao J, Zhang Z, Wu Y, Zhang L, Wu Z, Cheng P, et al. Impact of particle number and mass size
485 distributions of major chemical components on particle mass scattering efficiency in urban Guangzhou
486 in southern China. *Atmos. Chem. Phys.*, 19, 8471-8490, <https://doi.org/10.1021/es9810843>, 2019

487 Warneke, C., de Gouw, J. A., Edwards, P. M., Holloway, J. S., Gilman, J. B., Kuster, W. C., Graus, M.,
488 Atlas, E., Blake, D., Gentner, D. R., Goldstein, A. H., Harley, R. A., Alvarez, S., Rappenglueck, B.,

489 Trainer, M., and Parrish, D. D.: Photochemical aging of volatile organic compounds in the Los Angeles
490 basin: Weekday-weekend effect, *J. Geophys. Res.-Atmos.*, 118, 5018-5028,
491 <http://doi.org/10.1002/jgrd.50423>, 2013.

492 Wu, F., Chow, J. C., An, Z., Watson, J. G., and Cao, J.: Size-Differentiated Chemical Characteristics of
493 Asian Paleo Dust: Records from Aeolian Deposition on Chinese Loess Plateau, *J. Air Waste Manage.*,
494 61, 180-189, 10.3155/1047-3289.61.2.180, 2011.

495 Xu, H., Cao, J., Chow, J. C., Huang, R. J., Shen, Z., Chen, L. W. A., Ho, K. F., and Watson, J. G.: Inter-
496 annual variability of wintertime PM_{2.5} chemical composition in Xi'an, China: Evidences of changing
497 source emissions, *Sci. Total. Environ.*, 545, 546-555, <http://dx.doi.org/10.1016/j.scitotenv.2015.12.070>,
498 2016.

499 Xue, L., Wang, T., Louie, P. K. K., Luk, C. W. Y., Blake, D. R., and Xu, Z.: Increasing External Effects
500 Negate Local Efforts to Control Ozone Air Pollution: A Case Study of Hong Kong and Implications for
501 Other Chinese Cities, *Environ. Sci. Technol.*, 48, 10769-10775, 10.1021/es503278g, 2014.

502 Xue, L. K., Wang, T., Guo, H., Blake, D. R., Tang, J., Zhang, X. C., Saunders, S. M., and Wang, W. X.:
503 Sources and photochemistry of volatile organic compounds in the remote atmosphere of western China:
504 results from the Mt. Waliguan Observatory, *Atmos. Chem. Phys.*, 13, 8551-8567, 10.5194/acp-13-8551-
505 2013, 2013.

506 Xue, Y., Ho, S. S. H., Huang, Y., Li, B., Wang, L., Dai, W., Cao, J., and Lee, S.: Source apportionment
507 of VOCs and their impacts on surface ozone in an industry city of Baoji, Northwestern China, *Sci. Rep.-*
508 *UK.*, 7, 9979, <https://doi.org/10.1038/s41598-017-10631-4>, 2017.

509 Zhang, D. Z., Shi, G. Y., Iwasaka, Y., and Hu, M.: Mixture of sulfate and nitrate in coastal atmospheric
510 aerosols: individual particle studies in Qingdao (36 degrees 04 ' N, 120 degrees 21 ' E), China, *Atmos.*
511 *Environ.*, 34, 2669-2679, [http://doi.org/10.1016/s1352-2310\(00\)00078-9](http://doi.org/10.1016/s1352-2310(00)00078-9), 2000.

512 Zhang, D. Z., Zang, J. Y., Shi, G. Y., Iwasaka, Y., Matsuki, A., and Trochkin, D.: Mixture state of
513 individual Asian dust particles at a coastal site of Qingdao, China, *Atmos. Environ.*, 37, 3895-3901,
514 [http://doi.org/10.1016/s1352-2310\(03\)00506-5](http://doi.org/10.1016/s1352-2310(03)00506-5), 2003.

515 Zhang, N., Cao, J., Wang, Q., Huang, R., Zhu, C., Xiao, S., and Wang, L.: Biomass burning influences
516 determination based on PM_{2.5} chemical composition combined with fire counts at southeastern Tibetan
517 Plateau during pre-monsoon period, *Atmos. Res.*, 206, 108-116,
518 <https://doi.org/10.1016/j.atmosres.2018.02.018>, 2018.

519 Zhang, Q., Shen, Z., Cao, J., Zhang, R., Zhang, L., Huang, R. J., Zheng, C., Wang, L., Liu, S., Xu, H.,
520 Zheng, C., and Liu, P.: Variations in PM_{2.5}, TSP, BC, and trace gases (NO₂, SO₂, and O₃) between
521 haze and non-haze episodes in winter over Xi'an, China, *Atmos. Environ.*, 112, 64-71,
522 <https://doi.org/10.1016/j.atmosenv.2015.04.033>, 2015a.

523 Zhang, T., Cao, J. J., Tie, X. X., Shen, Z. X., Liu, S. X., Ding, H., Han, Y. M., Wang, G. H., Ho, K. F.,
524 Qiang, J., and Li, W. T.: Water-soluble ions in atmospheric aerosols measured in Xi'an, China: Seasonal
525 variations and sources, *Atmos. Res.*, 102, 110-119, <https://doi.org/10.1016/j.atmosres.2011.06.014>, 2011.

526 Zhang, Y., Wang, X., Zhang, Z., Lu, S., Huang, Z., and Li, L.: Sources of C-2-C-4 alkenes, the most
527 important ozone nonmethane hydrocarbon precursors in the Pearl River Delta region, *Sci. Total Environ.*,
528 502, 236-245, <https://doi.10.1016/j.scitotenv.2014.09.024>, 2015b.

529 Zhang, Y., Bao, F., Li, M., Chen, C., and Zhao, J.: Nitrate-Enhanced Oxidation of SO₂ on Mineral Dust:
530 A Vital Role of a Proton, *Environ. Sci. Technol.*, 53, 10139-10145, <https://doi.10.1021/acs.est.9b01921>,
531 2019.

532 Zhang, Z., Wang, X., Zhang, Y., Lü, S., Huang, Z., Huang, X., and Wang, Y.: Ambient air benzene at
533 background sites in China's most developed coastal regions: Exposure levels, source implications and
534 health risks, *Sci. Total Environ.*, 511, 792-800, <http://dx.doi.org/10.1016/j.scitotenv.2015.01.003>, 2015c.

535 Zheng Fang, W. D., Yanli Zhang, Xiang Ding, Mingjin Tang, Tengyu Liu, Qihou Hu, Ming Zhu, Zhaoyi
536 Wang, Weiqiang Yang, Zhonghui Huang, Wei Song, Xinhui Bi, Jianmin Chen, Yele Sun, Christian
537 George, and Xinming Wang: Open burning of rice, corn and wheat straws: primary emissions,
538 photochemical aging, and secondary organic aerosol formation, *Atmos. Chem. Phys.*, 17, 14821-14839,
539 <http://org/10.5194/acp-17-14821-2017>, 2017.

540 Zou, Y., Deng, X., Zhu, D., Gong, D., Wang, H., Li, F., Tan, H., Deng, T., Mai, B., and Liu, X.:
541 Characteristics of 1 year of observational data of VOCs, NO_x and O₃ at a suburban site in Guangzhou,
542 China, *Atmos. Chem. Phys.*, 15, 6625-6636, <https://doi.org/10.5194/acp-15-6625-2015>, 2015.

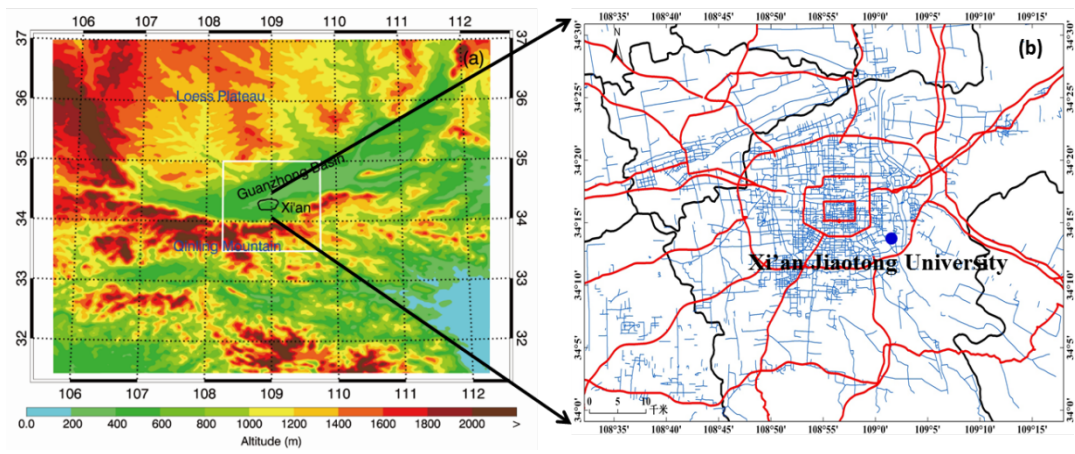
543



544

545

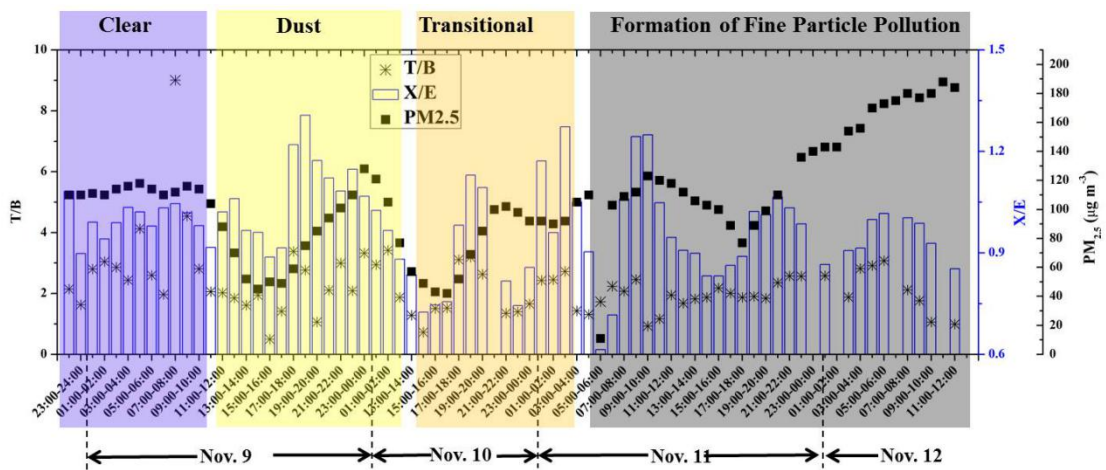
546
547
548
549
550
551
552
553
554
555
556
557
558
559
560
561
562



563
564
565
566
567
568

Figure 1: Regional and local maps of the study area, (a) Regional map showing the location of Xi'an and the surrounding geography; (b) local map of Xi'an showing the sampling site (blue dot), main roads (red lines), and secondary roads (blue lines).

569
 570
 571
 572
 573
 574
 575
 576
 577
 578
 579
 580
 581
 582
 583
 584
 585



586
 587
 588
 589
 590

Figure 2: Variations in the ratios of indicator volatile organic compound (VOC) species (toluene/benzene [T/B], and m,p-xylene/ethylbenzene [X/E]) and fine particle loadings during the study period.

591

592

593

594

595

596

597

598

599

600

601

602

603

604

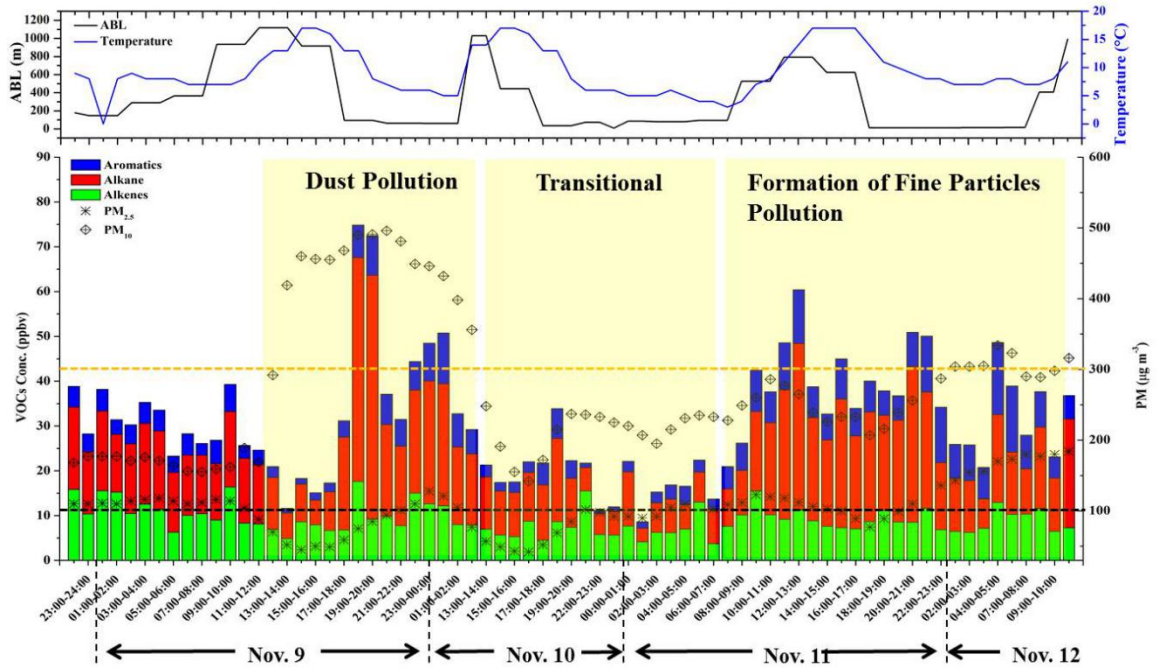
605

606

607

608

609



610

611 **Figure 3: Temporal variations in volatile organic compound (VOC) concentrations and particle levels during**
 612 **the sampling period (9–13 November 2016).**

613

614

615

616

617

618

619

620

621

622

623

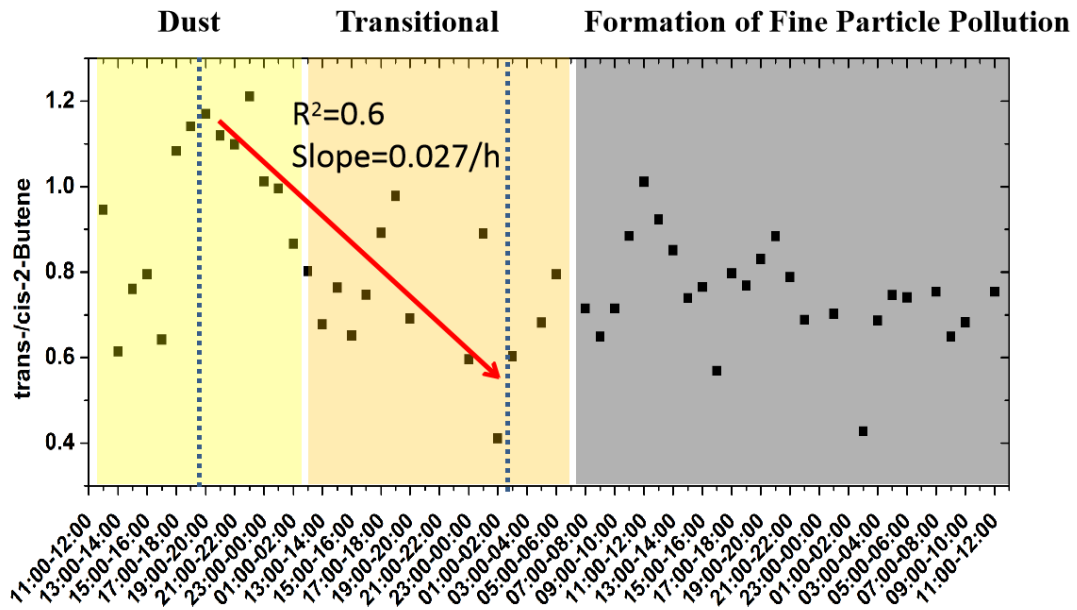
624

625

626

627

628



629

630 Figure 4: Temporal variation of trans-/cis-2-butene ratio in the dust-transitional-fine particle pollution period.

631

632

633

634

635

636

637

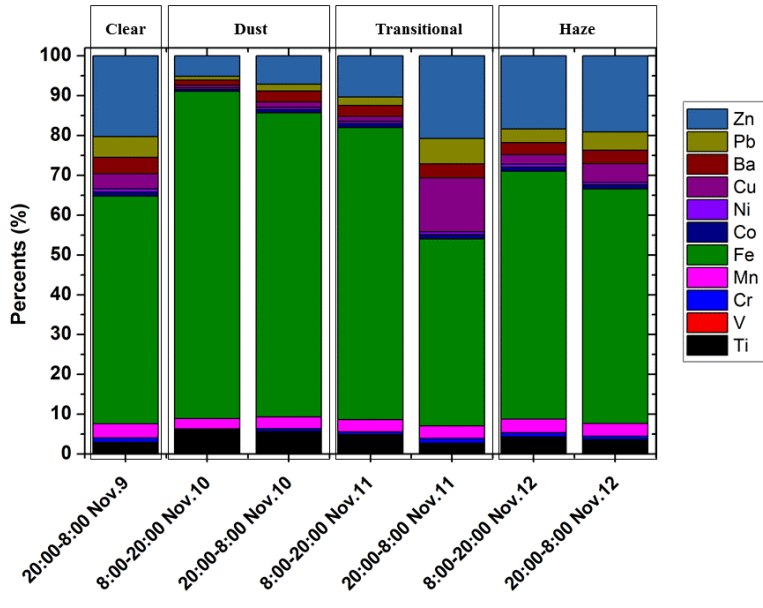
638

639

640

641

642



643

644 **Figure 5: Composition of selected metallic elements in the PM2.5 samples.**

645

646

647

648

649

650

651

652

653

654

655

656

657

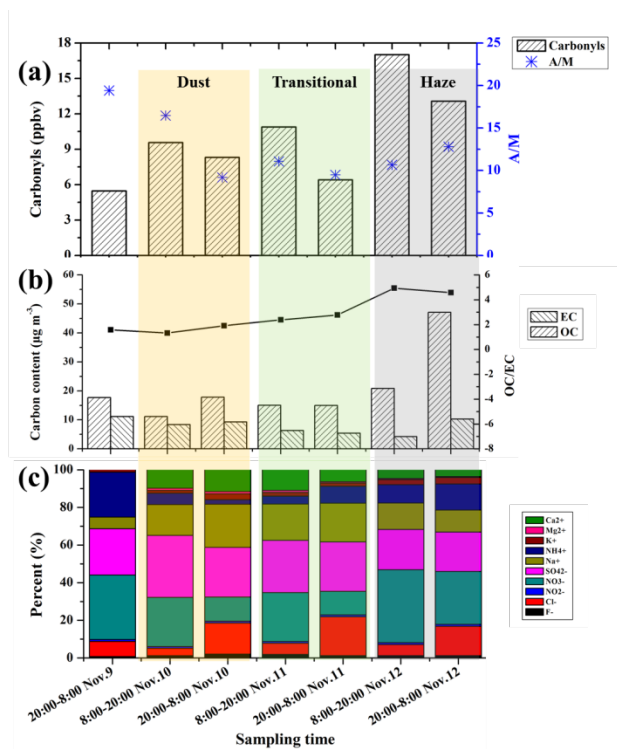
658

659

660

661

662



663

664 **Figure 6: Variations in (a) the mixing ratios of 17 carbonyl compounds and acetone to methylglyoxal (A/M)**
 665 **ratios in the gas phase, (b) particulate carbon fractions, (c) and particulate water-soluble ions during the**
 666 **study period.**

667

668

669

670

671